Available online at www.sciencedirect.com

ScienceDirect

Physics Letters B 647 (2007) 122–127

PHYSICS LETTERS B

www.elsevier.com/locate/physletb

Three-particle correlations from parton cascades in Au + Au collisions

G.L. Ma [a], Y.G. Ma [a,*], S. Zhang [a,b], X.Z. Cai [a], J.H. Chen [a,b], Z.J. He [a], H.Z. Huang [c], J.L. Long [a], W.Q. Shen [a], X.H. Shi [a,b], C. Zhong [a], J.X. Zuo [a,b]

[a] *Shanghai Institute of Applied Physics, Chinese Academy of Sciences, Shanghai 201800, China*
[b] *Graduate School of the Chinese Academy of Sciences, Beijing 100080, China*
[c] *Department of Physics and Astrophysics, University of California, Los Angeles, CA 90095, USA*

Received 21 August 2006; received in revised form 7 February 2007; accepted 7 February 2007

Available online 12 February 2007

Editor: W. Haxton

Abstract

We present a study of three-particle correlations among a trigger particle and two associated particles in Au + Au collisions at $\sqrt{s_{NN}} = 200$ GeV using a multi-phase transport model (AMPT) with both partonic and hadronic interactions. We found that three-particle correlation densities in different angular directions with respect to the triggered particle ('center', 'cone', 'deflected', 'near' and 'near-away') increase with the number of participants. The ratio of 'deflected' to 'cone' density approaches to 1.0 with the increasing of number of participants, which indicates that partonic Mach-like shock waves can be produced by strong parton cascades in central Au + Au collisions.

PACS: 25.75.-q; 24.10.Nz; 24.10.Pa; 25.75.Ld

Keywords: Three-particle correlation; Mach cone; Parton cascade; Hadronic rescattering; AMPT

1. Introduction

Ultra-relativistic heavy ion collisions may provide conditions sufficient for the formation of a deconfined plasma of quarks and gluons [1]. Experimental results from RHIC indicate that a strongly-interacting partonic matter (termed sQGP) has been created in the early stage of central Au + Au collisions at $\sqrt{s_{NN}} = 200$ GeV at RHIC [2]. Jet-like azimuthal correlation is one of the important hard probes to explore the natures of the newly formed matter. The disappearance [3] and re-appearance [4] of back-to-back high transverse momentum (p_T) particles from jets have been proved to result from the interactions between jet-partons and the hot and dense medium created in central Au + Au collisions. Recently, an interesting splitting of the away side peak has been observed in the di-hadron azimuthal angle ($\Delta\phi$) correlation distribution between soft associated particles and high p_T trigger particles in central Au + Au collisions at RHIC [5–7]. Such a double peak structure on the away-side is consistent with preferential conic emission of particles from jets and/or shock-wave induced collective motion from jet-medium interactions. We will refer to the observed double peaks on the away-side as the Mach-like structure without necessary implication on the dynamical mechanism.

Several theoretical interpretations about the Mach-like structure have been proposed. For instances, Stöcker et al. proposed the Mach-like structure from jets traversing the dense medium as a probe of the equation of state (EOS) and the speed of sound in the medium [8]. Casalderrey-Solana and Shuryak et al. argued a shock wave generation because jets travel faster than the sound in the medium [9]. They fitted the broad splitting structure on the away side in di-hadron azimuthal correlation with a Mach-cone shock wave mechanism. Vitev has shown that the cancellation of collinear bremsstrahlung in QCD medium can lead to large angle emission of gluons [10]. Koch and Wang et al. used a Cherenkov radiation model with negative dispersion relation to produce the Mach-like structure [11]. In

* Corresponding author.
E-mail address: ygma@sinap.ac.cn (Y.G. Ma).

0370-2693
doi:10.1016/j.physletb.2007.02.008

Ref. [12], Armesto proposed that the medium-induced gluon radiation could be affected by the collective flow in the medium. It has also been argued by Müller et al. that a Mach-like structure can appear via the excitation of collective plasmon waves by moving color charges associated with the leading jet [13]. Renk and Ruppert found that in order to reproduce the experimental data a large fraction (about 90%) of the lost energy of jet has to be channelled to excite a shock wave in a dense medium at a soft point of EOS [14]. Satarov et al. investigated Mach shocks induced by partonic jets in expanding quark-gluon plasma [15]. However, Chaudhuri and Heinz reported no observation of Mach-like structures in di-hadron $\Delta\phi$ correlations from jet quenching dynamically in a hydrodynamic QGP fluid [16]. A consistent dynamical picture for the generation of the Mach-like structure in particle correlations has yet to emerge and further investigations are needed.

In order to shed light on the puzzle of the dynamical origin of the splitting structure on the away-side, three-particle correlation has been proposed to look at the multi-particle correlation in the emission pattern of particles. The di-hadron correlation cannot distinguish different emission scenarios since correlation only deals between emitted and the trigger particle. However the three-particle correlation is capable of distinguishing the different scenarios when simultaneous emission of two particles are investigated with the trigger particle. If the splitting structure of away-side is from large angle gluon emission or deflection due to strong collective flow in an event, the two associated particles will be clustered in a narrow cone on a single-side of the away-jet direction. However, if the production mechanism is Mach-cone shock wave or Cherenkov gluon radiation, the partons in the shock-wave front or Cherenkov gluons will be emitted conically around the away-side jet center in single event. In this case, the two associated particles can be simultaneously on both sides of the $\Delta\phi = \phi_{\rm assoc} - \phi_{\rm trig}$ distribution with respect to the opposite direction of the trigger particle. Experimental studies of the three-particle correlations have been reported by both the STAR [17–19] and the PHENIX [20] collaborators.

In our previous work, we reported observation of Mach-like structure in di-hadron correlations from Au + Au collisions using a multi-phase transport model (AMPT) where both partonic and hadronic interactions are included [21]. Both parton cascades and hadronic rescatterings can produce apparent di-hadron correlations with Mach-like structures. But the hadronic rescattering mechanism alone cannot reproduce the observed experimental amplitude of Mach-like structure on the away-side, which indicates that parton cascade processes are indispensable. However, detailed dynamical mechanisms for the Mach-like structure still await to be determined. In this Letter, we present a study of three-particle correlation among one trigger particle and two associated particles in Au + Au collisions at $\sqrt{s_{NN}} = 200$ GeV with the AMPT model. Three particle correlations in regions of azimuthal angular directions of 'cone', 'deflected', 'center', 'near' and 'near-away', which will be defined later, will be presented for Au + Au collisions from AMPT. With decreasing number of participants, 'center' correlations become more dominant, and 'cone' and 'deflected' correlations seem to disappear. Our results indicate that the three-particle correlations in central collisions are mainly produced by partonic Mach-like shock wave effect, while in peripheral collisions deflected jet effect also contributes to the Mach-like structure. Effects of hadronic rescatterings and parton cascades on three-particle correlation are also investigated.

2. Brief description of the AMPT model

AMPT model [22] is a hybrid model which consists of four main processes: the initial conditions, partonic interactions, the conversion from partonic matter into hadronic matter and hadronic interactions. The initial conditions, which include the spatial and momentum distributions of minijet partons and soft string excitations, are obtained from the HIJING model [23]. The excitation of strings will melt strings into partons. Scatterings among partons are modelled by Zhang's parton cascade model (ZPC) [24], which at present includes only two-body scatterings with cross section obtained from pQCD calculation with screening mass. In the default version of AMPT model (we briefly call it as "the default AMPT" model) [25], partons are recombined with their parent strings when they stop interactions, and the resulting strings are converted to hadrons using the Lund string fragmentation model [26]. In the string melting version of the AMPT model (we briefly call it as "the melting AMPT" model) [27], a quark coalescence model is used to combine partons to form hadrons. Dynamics of the subsequent hadronic matter is then described by A Relativistic Transport (ART) model [28]. Details of the AMPT model can be found in a recent review [22]. Previous studies [22,27,29] demonstrated that the partonic effect cannot be neglected and the melting AMPT model is much more appropriate than the default AMPT model in describing nucleus–nucleus collisions at RHIC. In the present work, the parton interaction cross section in the AMPT model is assumed to be 10 mb consistent with previous calculations [22,29].

3. Analysis method

The mixing-event technique has been used in our three-particle correlation analysis. The p_T window cuts for trigger and associated particles were selected as $2.5 < p_T^{\rm trig} < 4$ GeV/c and $1.0 < p_T^{\rm assoc} < 2.5$ GeV/c, respectively. Both trigger and associated particles were required to be within a pseudo-rapidity window of $|\eta| < 1.0$, where η is the pseudo-rapidity of hadrons in the center-of-mass frame of Au + Au collisions. In the same events, raw 3-particle correlation signals in $\Delta\phi_1 = \phi_1 - \phi_{\rm trig}$ versus $\Delta\phi_2 = \phi_2 - \phi_{\rm trig}$ were histogrammed. Fig. 1(a) shows the raw 3-particle correlation distribution in the top 10% central Au + Au collisions at $\sqrt{s_{NN}} = 200$ GeV in the melting AMPT model with hadronic rescattering. Three classes of background contributions are expected to contribute to the raw signal. The first one is the hard-soft background which comes from a jet-induced trigger-associated pair combined with a background associated particle from bulk medium. We reproduced it by mixing a trigger-associated pair with another associated particle from a different event (Fig. 1(b)).

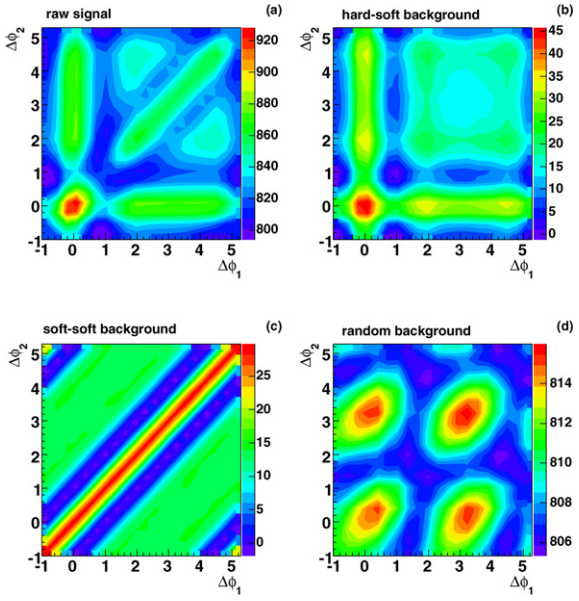

Fig. 1. Three-particle correlations in the top 10% central Au + Au collisions at $\sqrt{s_{NN}} = 200$ GeV from the melting AMPT model with hadronic rescattering. (a): Raw signal. (b): Hard-soft background. (c): Soft-soft background. (d): Random background.

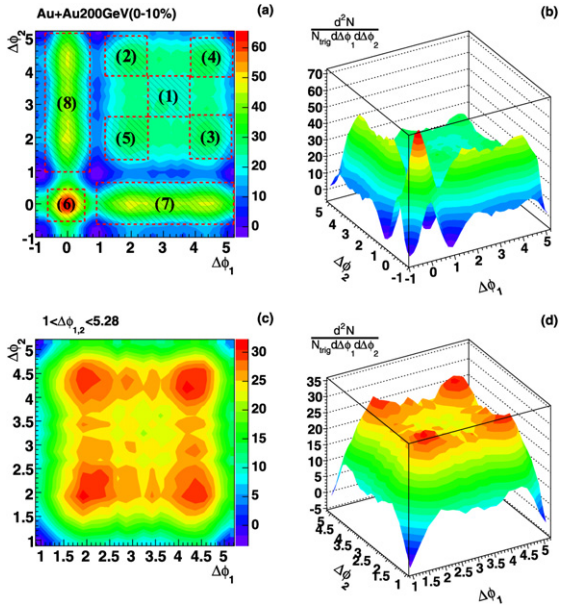

Fig. 2. Background subtracted 3-particle correlations in the top 10% central Au + Au collisions at $\sqrt{s_{NN}} = 200$ GeV for the melting AMPT model with hadronic rescattering. (a) and (b): Background subtracted 3-particle correlations ($-1 < \Delta\phi_{1,2} < 5.28$); (c) and (d): background subtracted 3-particle correlations ($1 < \Delta\phi_{1,2} < 5.28$) from the selected regions (1, 2, 3, 4, 5). The azimuthal angular regions are defined in panel (a)–(1): 'center' region; (2) and (3): 'cone' regions; (4) and (5): 'deflected' regions; (6): 'near' region; (7) and (8): 'near-away' regions.

The second one is soft–soft background which comes from an associated particle pair combined with an uncorrelated trigger particle. We constructed this background by mixing an associated particle pair from one event with a trigger particle from a different event (Fig. 1(c)). The third one is a random combinatorial background, which was produced by mixing a trigger particle and two associated particles respectively from three different events (Fig. 1(d)). We required that the mixed events are all from very close collision centralities which can be determined by impact parameters in simulations. In order to subtract the backgrounds from the raw signals, we set the signal at $0.8 < |\Delta\phi_{1,2}| < 1.2$ to be zero. Fig. 2(a) and (b) give background subtracted 3-particle correlations in the top 10% central Au + Au collisions at $\sqrt{s_{NN}} = 200$ GeV in the melting AMPT model which includes hadronic rescattering. In order to observe the 3-particle correlations among a trigger particle and two away-side associated particles clearly, the 3-particle correlations in $1 < \Delta\phi_{1,2} < 5.28$ region are shown with an expanded scale in Fig. 2(c) and (d).

4. Results and discussions

We divide the three-particle correlation distribution into several regions based on the possible origin of the particle emission pattern as shown in Fig. 2(a). The first one is 'center' region ($|\Delta\phi_{1,2} - \pi| < 0.5$) where the three-particle correlation mainly comes from one trigger particle and two associated particles in the center of away side. The 'center' correlations represent penetration ability of away-side jet. The second one is 'cone' region ($|\Delta\phi_1 - (\pi \pm 1)| < 0.5$ and $|\Delta\phi_2 - (\pi \mp 1)| < 0.5$) where three-particle correlation would form splitting peaks in di-hadron $\Delta\phi$ correlation due to a conical emission pattern from away-side jet. It was predicted that this conical emission may be produced by a Mach-cone shock wave effect when a jet propagates faster than the speed of sound in the medium creating shock wave front in the cone region. The third one is 'deflected' region ($|\Delta\phi_{1,2} - (\pi \pm 1)| < 0.5$) where associated particles are emitted in the same side-ward region of the away-side jet in one event. The 'deflected' region three-particle correlations can also yield splitting peaks on the away-side of two-particle correlation distribution because though within one event the away-side jet is deflected to one side only, but inclusively with many events both sides of the jet direction can be populated. The fourth region is the 'near' area ($|\Delta\phi_{1,2}| < 0.5$) where three-particle correlation represents the correlation among trigger particle and associated particles on near side of the trigger direction. The fifth one is 'near-away' correlation region ($1 < \Delta\phi_{1,2} < 5.28$ and $|\Delta\phi_{2,1}| < 0.5$), which reflects the correlation among trigger particle, one associated particle on near side and another associated particle on away side. The five regions have been marked with different numbers in panel (a) of Fig. 2 for clarity. We will examine three-particle correlations in the above five regions.

Fig. 3 shows three-particle correlation distribution in the ($1 < \Delta\phi_{1,2} < 5.28$) area from Au + Au collisions at $\sqrt{s_{NN}} =$ 200 GeV with different centralities using the melting AMPT model, and $p + p$ collisions at $\sqrt{s_{NN}} = 200$ GeV using the default AMPT model before and after hadronic rescattering. Here we chose the default AMPT model to simulate $p + p$ collisions at $\sqrt{s_{NN}} = 200$ GeV, since the string melting mechanism has little effect on $p + p$ collisions which has also been demonstrated previously [22]. Three-particle correlations in all 'center', 'deflected' and 'cone' regions can be observed in cen-

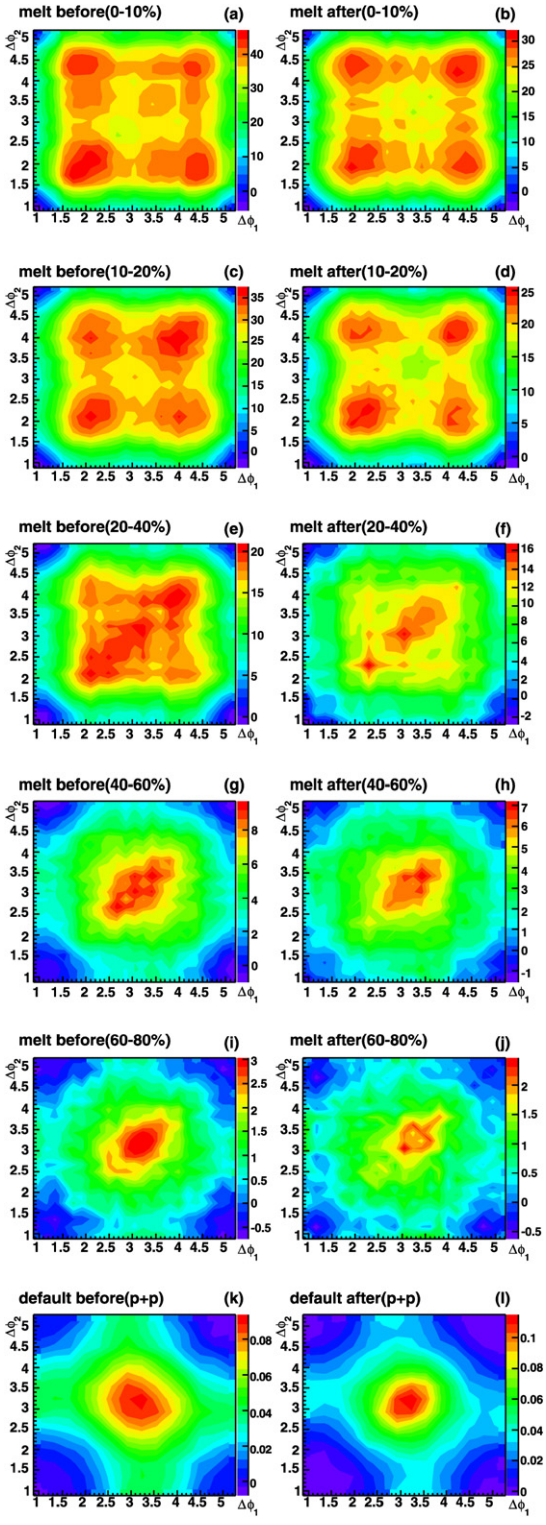

Fig. 3. Background subtracted segmental 3-particle correlation areas ($1 < \Delta\phi_{1,2} < 5.28$) in different centralities in Au + Au collisions at $\sqrt{s_{NN}} = 200$ GeV in the melting AMPT model ((a)–(j)), as well as $p + p$ collisions at $\sqrt{s_{NN}} = 200$ GeV in the default AMPT model ((k)–(l)). The left column from (a) to (k) shows the results before hadronic rescattering (briefly named as "melt before" or "default before") and the right column from (b) to (l) shows the results after hadronic rescattering (briefly named as "melt after" or "default after"). (a) and (b): 0–10%; (c) and (d): 10–20%; (e) and (f): 20–40%; (g) and (h): 40–60%; (i) and (j): 60–80%. (k) and (l): $p + p$ collisions.

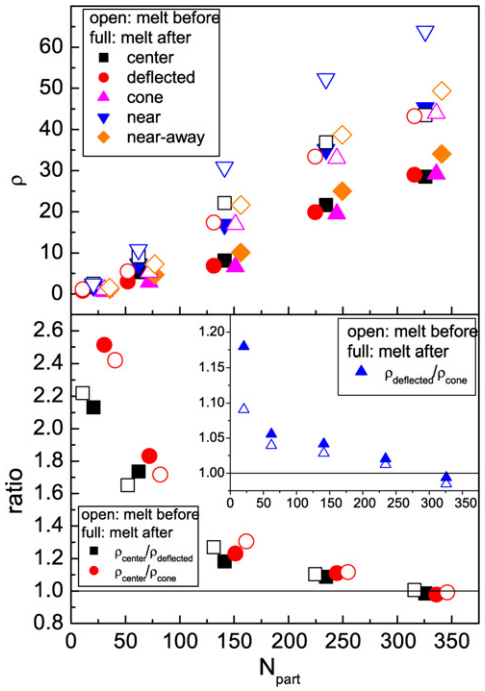

Fig. 4. The correlation density analysis for Au + Au collisions at $\sqrt{s_{NN}} = 200$ GeV in the melting AMPT model before and after hadronic rescattering. Top panel: the average three-particle correlation densities ρ at different regions as a function of N_{part}; Bottom panel: ratios of average three-particle correlation density ('center'/'deflected' and 'center'/'cone') as a function of N_{part}; The insert of the bottom panel: ratio of average three-particle correlation density ('deflected'/'cone') as a function of N_{part}. Note that some points have been shifted slightly in N_{part} axis for clarity.

tral Au + Au collisions with the melting AMPT model regardless of the inclusion of hadronic rescatterings. As the collisions become more peripheral, the 'deflected' and 'cone' region correlations gradually disappear until only the 'center' correlations remain in the most peripheral Au + Au collisions and $p + p$ collisions.

In order to quantitatively express three-particle correlation strength in these different regions, region-averaged three-particle correlation density ρ is defined according to the following equation:

$$\rho = \frac{\iint_{\text{region}} \frac{d^2N}{N_{\text{trig}}\, d\Delta\phi_1\, d\Delta\phi_2}\, d\Delta\phi_1\, d\Delta\phi_2}{\iint_{\text{region}} d\Delta\phi_1\, \Delta\phi_2}. \tag{1}$$

The top panel of Fig. 4 shows three-particle correlation densities ρ in different regions as a function of N_{part} (number of participants) for Au + Au collisions at $\sqrt{s_{NN}} = 200$ GeV in the melting AMPT model before and after hadronic rescattering.

Our results show that three-particle correlation densities decrease after hadronic rescattering process, which indicates hadronic rescatterings could weaken three-particle correlation strength. However di-hadron correlation is almost unchanged in this p_T window selection in our previous work [21]. Such a difference is indicative of enhanced sensitivity to hadronic rescatterings in the three-particle correlations in comparison to the di-hadron correlations.

The bottom panel of Fig. 4 shows the centrality dependences of two ratios, namely the density ratios of 'center'/'deflected' and 'center'/'cone', in Au+Au collisions at $\sqrt{s_{NN}} = 200$ GeV. Both ratios fall from above 2.0 in peripheral collisions to near 1.0 in central collisions with the increasing of $N_{\rm part}$, which indicates that the strengths of particle emission in the 'cone' and in the 'deflected' regions increase dramatically in central collisions relative to the particles in the 'center' region. Since the 'center' correlation reflects the ability of '*punch–through*' for the backward jet, our results indicate that the backward jet can maintain the original jet direction well in peripheral collisions while in central collisions many particles are emitted in the 'cone' and the 'deflected' directions, away from the original jet direction.

In the insert of Fig. 4, the ratio of 'deflected'/'cone' slightly decreases with $N_{\rm part}$ and approaches 1.0 in central collisions. The Mach-cone shock wave and the Cherenkov gluon radiation scenarios predicted almost equal strength in the three-particle correlations in the 'deflected' $(\pi \pm D, \pi \pm D)$ and 'cone' $(\pi \pm D, \pi \mp D)$ regions, where D is the splitting parameter of away side (i.e. half distance between two peaks on away side in di-hadron $\Delta\phi$ correlation function). Our observed three-particle correlations in the central Au + Au collisions from the AMPT model are consistent with these model predictions. Such a consistency may be related to the hydrodynamic-like behavior in the AMPT model due to strong parton–parton couplings and interactions.

More comments on the origin of the three-particle correlations in the AMPT model are in order. The melting AMPT model was shown to produce good descriptions of elliptic flow of identified hadrons and even yielded the correct mass ordering of elliptic flow [27,29], which has been considered an important feature of hydrodynamics models. Such an agreement can be attributed to the large parton–parton interaction cross section in the AMPT model, which leads to strong parton cascades that couples partons together inducing the onset of hydrodynamical behavior [30]. However, in another hydrodynamic model [16] the signal of Mach-cone shock waves can hardly be observed in the di-hadron correlations. It appears that the large strength of parton cascades and coupling of partons as described in the AMPT model bring about the conic emission pattern on the away-side prominently. The linearized hydrodynamical approximation may not be adequate for the strong jet-medium interaction region where the medium also experiences rapid variation of energy density and without sufficient thermalization [9]. On the other hand, the observed three-particle correlations may partly stem from deflected jets (represented by $\frac{\rho_{\rm deflected}}{\rho_{\rm cone}} - 1$) in peripheral collisions where 'center' correlation becomes dominated. In the AMPT model there is no inclusion of large angle gluon bremsstrahlung mechanism [10] which may also play a role in real collisions. In addition, we note that the backward jet may also be distributed over a wide rapidity range [10,31] beyond our narrow η window cut. In our model, we used LO pQCD cross sections from HIJING model for the minijet production, which has successfully described the suppression of back-to-back jets [32]. Our selection of the η window cut was to match the detector acceptance of the RHIC experiments.

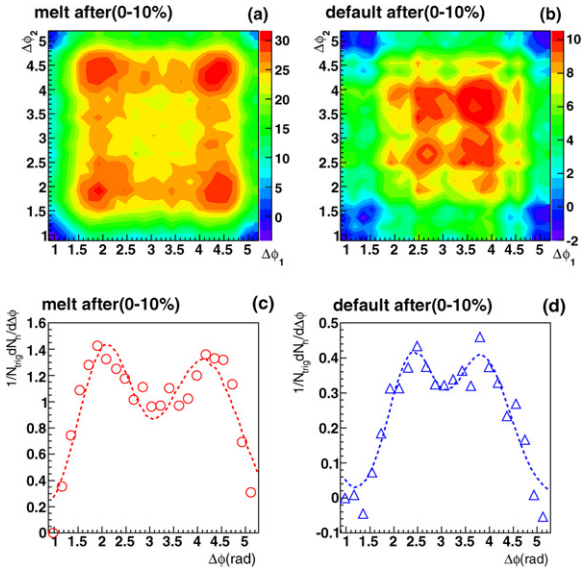

Fig. 5. Background subtracted three-particle correlations in selected $(1 < \Delta\phi_{1,2} < 5.28)$ regions ((a) and (b)) and away-side di-hadron correlations ((c) and (d)) in the top 10% Au + Au collisions at $\sqrt{s_{NN}} = 200$ GeV in the melting AMPT model (left column) and the default AMPT model (right column) after hadronic rescattering.

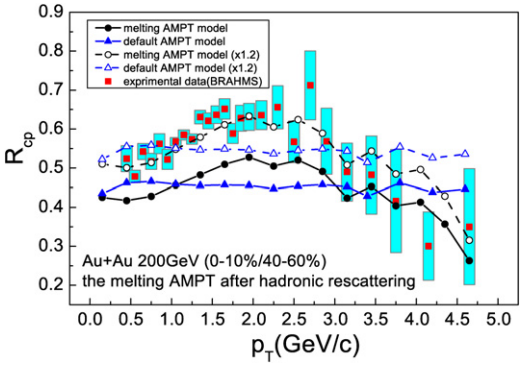

Fig. 6. The p_T dependences of nuclear modification factor R_{cp} of charge hadrons for 0–10%/40–60% in Au + Au collisions at $\sqrt{s_{NN}} = 200$ GeV in the melting and default AMPT model with hadronic rescattering. The experimental data come from Ref. [33].

In addition, we studied the effect of parton cascades on three-particle and di-hadron correlation by comparing the results of the default AMPT model and the melting AMPT model. Fig. 5(a) and (b) give three-particle correlations in selected $(1 < \Delta\phi_{1,2} < 5.28)$ regions for the melting AMPT model and the default AMPT model. Note both cases are the results after hadronic rescattering in the top 10% Au + Au collisions at $\sqrt{s_{NN}} = 200$ GeV. Though with large statistical errors, the default AMPT model seems to produce a three-particle correlation, but the three-particle correlation area is considerably less than that from the melting AMPT model. It is consistent with the results of di-hadron correlation in our previous work (see Fig. 5(c) and (d)) that concluded that hadronic rescattering alone cannot reproduce a splitting parameter of Mach-like structure on away side large enough to match the experimental measurements [21].

The nuclear modification factor, R_{cp}, is also considered a useful probe of the energy loss of high p_T partons in the dense medium created in nucleus–nucleus collisions. Fig. 6 shows the transverse momentum dependences of nuclear modification factor R_{cp} of charge hadrons in the melting and default AMPT model with hadronic rescattering. The R_{cp} is defined by following formula:

$$R_{cp} = \frac{N_{\text{bin}}|_P}{N_{\text{bin}}|_C} \times \frac{\frac{d^2N}{p_T\,dp_T\,d\eta}\big|_C}{\frac{d^2N}{p_T\,dp_T\,d\eta}\big|_P},$$

where the central and the peripheral collision centralities are 0–10% and 40–60%, and the respective number of binary collisions $N_{\text{bin}} = 939.4$ (0–10%), 93.7 (40–60%). The R_{cp} in the melting AMPT model is of similar shape of experimental data, which can match experimental data well if scaled by a factor 1.2. However the R_{cp} from the default AMPT model seems to be independent of p_T and inconsistent with experimental data. The partonic interactions in the melting AMPT model appear essential to describe the shape of nuclear modification factor as a function of p_T in Au + Au collisions. Furthermore, R_{cp} is suppressed more heavily in higher p_T range ($p_T > 3.5$ GeV/c) in the melting AMPT model than in the default AMPT model, which may indicate that more energies are lost into the medium by parton cascade mechanism especially for high p_T particles, which is expected to be in favor of the formation of partonic Mach-like shock waves.

5. Conclusions

Three-particle correlations have been extracted by using event-mixing technique in a multi-phase transport model with both partonic and hadronic interactions. Correlations in different azimuthal angular regions with respect to the trigger jet direction, so-called 'center', 'deflected', 'cone', 'near' and 'near-away', have been discussed for Au + Au collisions at $\sqrt{s_{NN}} =$ 200 GeV. The AMPT results with and without hadronic rescattering are also compared. The 'center' three-particle correlation becomes more and more dominant with the decreasing of number of participants, which may reflect the centrality dependence of partonic density and the strength of partonic interactions. The density ratio of 'deflected'/'cone' approaching 1.0 in central collisions indicates that the three-particle correlation in central collisions is mainly produced by a partonic Mach-like shock wave mechanism, and in peripheral collisions deflected jet mechanism also contributes. The partonic Mach-like shock wave mainly originates from strong partonic interactions in dense partonic matter. The three-particle correlations are also sensitive to hadronic rescatterings, therefore the effect of hadronic rescattering may need to be considered in quantitative studies. The default AMPT model, where only the hadronic rescattering mechanism plays a dominant role, produces a three-particle correlation area much smaller than the melting AMPT model which includes both parton cascade and hadron rescattering mechanisms. Our AMPT calculation of three-particle correlations re-affirms our previous conclusion from di-hadron correlation studies that hadronic rescattering alone cannot produce an amplitude of Mach-like cone on away side large enough to match the experimental data. Parton cascade mechanism is essential and important in order to describe the amplitude of observed experimental Mach-like structure.

Acknowledgements

This work was supported in part by the National Natural Science Foundation of China under Grant Nos. 10610285 and 10328259, the Knowledge Innovation Project of Chinese Academy of Sciences under Grant No. KJCX2-YW-A14 and KJXC3-SYW-N2, and the Shanghai Development Foundation for Science and Technology under Grant Numbers 05XD14021 and 06JC14082.

References

[1] F. Karsch, Nucl. Phys. A 698 (2002) 199c.
[2] I. Arsene, et al., BRAHMS Collaboration, Nucl. Phys. A 757 (2005) 1; B.B. Back, et al., PHOBOS Collaboration, Nucl. Phys. A 757 (2005) 28; J. Adames, et al., STAR Collaboration, Nucl. Phys. A 757 (2005) 102; S.S. Adler, et al., PHENIX Collaboration, Nucl. Phys. A 757 (2005) 184.
[3] J. Adams, et al., STAR Collaboration, Phys. Rev. Lett. 91 (2003) 072304.
[4] J. Adams, et al., STAR Collaboration, Phys. Rev. Lett. 97 (2006) 162301.
[5] J.G. Ulery, STAR Collaboration, Nucl. Phys. A 774 (2006) 581.
[6] S. Adler, et al., PHENIX Collaboration, Phys. Rev. Lett. 97 (2006) 052301.
[7] J. Jia, PHENIX Collaboration, nucl-ex/0510019.
[8] H. Stöcker, Nucl. Phys. A 750 (2005) 121.
[9] J. Casalderrey-Solana, et al., J. Phys. Conf. Ser. 27 (2005) 22; J. Casalderrey-Solana, et al., Nucl. Phys. A 774 (2006) 577, hep-ph/0602183.
[10] I. Vitev, Phys. Lett. B 630 (2005) 78.
[11] V. Koch, A. Majumder, X.-N. Wang, Phys. Rev. Lett. 96 (2006) 172302.
[12] N. Armesto, C.A. Salgado, U.A. Wiedemann, Phys. Rev. Lett. 93 (2004) 242301.
[13] J. Ruppert, B. Müller, Phys. Lett. B 618 (2005) 123.
[14] T. Renk, J. Ruppert, Phys. Rev. C 73 (2006) 011901(R).
[15] L.M. Satarov, H. Stöcker, I.N. Mishustin, Phys. Lett. B 627 (2005) 64.
[16] A.K. Chaudhuri, U. Heinz, Phys. Rev. Lett. 97 (2006) 062301.
[17] J.G. Ulery, F. Wang, nucl-ex/0609016; J.G. Ulery, F. Wang, nucl-ex/0609017.
[18] C.A. Pruneau, Phys. Rev. C 74 (2006) 064910.
[19] J.G. Ulery, STAR Collaboration, nucl-ex/0609047.
[20] N. Ajitanand, PHENIX Collaboration, nucl-ex/0609038.
[21] G.L. Ma, S. Zhang, Y.G. Ma, et al., Phys. Lett. B 641 (2006) 362.
[22] Z.W. Lin, C.M. Ko, B.A. Li, B. Zhang, S. Pal, Phys. Rev. C 72 (2005) 064901.
[23] X.-N. Wang, M. Gyulassy, Phys. Rev. D 44 (1991) 3501; M. Gyulassy, X.-N. Wang, Comput. Phys. Commun. 83 (1994) 307.
[24] B. Zhang, Comput. Phys. Commun. 109 (1998) 193.
[25] B. Zhang, C.M. Ko, et al., Phys. Rev. C 61 (2000) 067901.
[26] B. Andersson, G. Gustafson, et al., Phys. Rep. 97 (1983) 31.
[27] Z.W. Lin, C.M. Ko, Phys. Rev. C 65 (2002) 034904; Z.W. Lin, C.M. Ko, et al., Phys. Rev. Lett. 89 (2002) 152301.
[28] B.A. Li, C.M. Ko, Phys. Rev. C 52 (1995) 2037.
[29] J.H. Chen, Y.G. Ma, G.L. Ma, et al., Phys. Rev. C 74 (2006) 064902.
[30] B. Zhang, M. Gyulassy, C.M. Ko, Phys. Lett. B 455 (1999) 45.
[31] T. Renk, J. Ruppert, hep-ph/0605330.
[32] X.-N. Wang, Phys. Lett. B 595 (2004) 165.
[33] I. Arsene, et al., BRAHMS Collaboration, Phys. Rev. Lett. 91 (2003) 072305.